Front. Earth Sci. 2018, 12(3): 583–599
https://doi.org/10.1007/s11707-017-0684-6

RESEARCH ARTICLE

Upriver transport of dissolved substances in an estuary and sub-estuary system of the lower James River, Chesapeake Bay

Bo HONG (✉)[1], Jian SHEN[2], Hongzhou XU[3]

1 School of Civil and Transportation Engineering, South China University of Technology, Guangzhou 510641, China
2 Virginia Institute of Marine Science, College of William & Mary, Williamsburg VA23062, USA
3 Institute of Deep-sea Science and Engineering, Chinese Academy of Sciences, Sanya 572000, China

Abstract The water exchange between the James River and the Elizabeth River, an estuary and sub-estuary system in the lower Chesapeake Bay, was investigated using a 3D numerical model. The conservative passive tracers were used to represent the dissolved substances (DS) discharged from the Elizabeth River. The approach enabled us to diagnose the underlying physical processes that control the expansion of the DS, which is representative of potential transport of harmful algae blooms, pollutants from the Elizabeth River to the James River without explicitly simulating biological processes. Model simulations with realistic forcings in 2005, together with a series of process-oriented numerical experiments, were conducted to explore the correlations of the transport process and external forcing. Model results show that the upriver transport depends highly on the freshwater discharge on a seasonal scale and maximum upriver transport occurs in summer with a mean transport time ranging from 15–30 days. The southerly/easterly wind, low river discharge, and neap tidal condition all act to strengthen the upriver transport. On the other hand, the northerly/westerly wind, river pulse, water level pulse, and spring tidal condition act to inhibit the upriver transport. Tidal flushing plays an important role in transporting the DS during spring tide, which shortens the travel time in the lower James River. The multivariable regression analysis of volume mean subtidal DS concentration in the mesohaline portion of the James River indicates that DS concentration in the upriver area can be explained and well predicted by the physical forcings ($r = 0.858$, $p = 0.00001$).

Keywords transport process, physical forcing, numerical modeling, estuary, Chesapeake Bay

Received June 20, 2017; accepted October 25, 2017

E-mail: bohong@scut.edu.cn

1 Introduction

The James River is a western tributary of the lower Chesapeake Bay (Fig. 1(a)). This river is distinguished by a meandering main channel. An abrupt bend of the river occurs at Newport News Point (NNP), approximately 10.5 km from its mouth, where the orientation of the river changes from northeast-southwest in the lower river to southeast-northwest in the upper river. Hampton Flats is the shoal flanking the northern side of the deep channel in the lower James River. Water depth over the Hampton Flats is less than 5 m. The Elizabeth River, a heavily industrialized waterway, is one of the important tributaries that enter the lower James River.

The study of Morse et al. (2011) showed that the Elizabeth River and one of its branches, Lafayette River, acted as initiation regions for the algal bloom in the James River during the summers of 2007 and 2008. After the bloom of *C. polykrikoides* appeared in the Lafayette River and Elizabeth River, phytoplankton was transported from these regions into the lower James River. The phytoplankton was then transported upriver by local estuarine circulation and formed massive blooms over large portions of the tidal James River and lower Chesapeake Bay. Being a heavily industrialized waterway, the Elizabeth River could be a source ground that injects pollutant contaminants, nutrients, etc. to the lower James River. Although the origin of the bloom was shown by both *in situ* observations and numerical modeling in Morse et al. (2011), physical processes that control the temporal-spatial variations of the concentration and the extent of upriver transport of dissolved substances (DS) in the James River have not been fully assessed. Understanding the physical processes that modulate the transport of DS from the Elizabeth River to the James River is necessary in order to

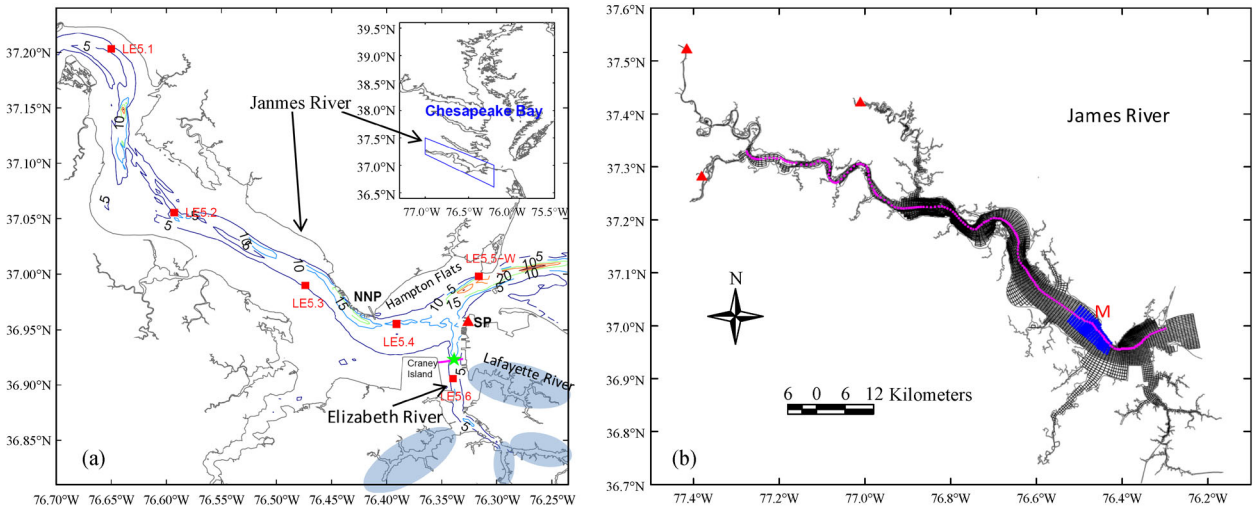

Fig. 1 (a) The topography of the James River. The water depth is in meters. The contour interval is 5 m. The transect across the mouth of the Elizabeth River is marked. The star at the mouth of the Elizabeth River denotes the position where the exchange flow was calculated in Figs. 5–9. The Sewells Point (SP) Station is marked by a red triangle. Stations LE5.1, LE5.2, LE5.3, LE5.4, LE5.5-W, and LE5.6 are marked by red squares. The four major branches of the Elizabeth River are marked by the shaded areas; (b) Computational domain and model grid of the James River. The three red triangles represent the locations of the freshwater input. The transect along the main channel of the James River is marked. The domain M is selected as a representative region for the analysis of upstream transport.

assess the biochemical and ecological status and human impacts in this estuary and sub-estuary system.

The James River estuary is a micro-tidal, partially mixed estuary with well-developed estuarine circulation forced by freshwater discharge and tides (Shen and Lin, 2006). Tides are predominantly semidiurnal with fortnightly variability between neap and spring tides, generating differences in the baroclinic pressure gradients, advective accelerations, and friction (Valle-Levinson et al., 2000). The maximum tidal amplitudes are 0.45 m and 0.20 m during spring and neap cycles, respectively (Basdurak and Valle-Levinson, 2013). The transport and distribution of DS are controlled by estuarine circulation. The hydrodynamic conditions in the lower portion of the James River are complex. Both observations (Kuo et al., 1990; Brubaker and Simpson, 1999) and modeling studies (Shen et al., 1999) provided evidence for the tidally driven development of a counterclockwise eddy in the lower James River. The northern part of the eddy occupies the flanking area of Hampton Flats and flows towards the NNP. A strong tidal front develops off NNP (Kuo et al., 1988). As this tidal intrusion front advances up the estuary during the flooding tide, prominent and consistent features in the velocity field include a localized zone of convergent flow beneath the stratified shear layer just upriver of the front (Brubaker and Simpson, 1999). Numerical experiments of Shen et al. (1999) proved that saltier, denser water from Hampton Flats submerges below the fresher, less dense water at the frontal boundary off NNP and the DS in the water from Hampton Flats was entrained into the lower part of the water column, where they are transported upriver due to estuarine circulation. Such a mechanism may enhance the upriver transport of DS and allow for a greater spatial expansion of blooms than what is possible due to the typical upriver transport during flood tide. However, previous numerical studies were conducted under idealized conditions and focused on the front area. The exchange between estuary and sub-estuary under various hydrodynamic conditions with respect to local and remote effects has not been fully studied.

In this study, we investigate the upriver transport of DS that enters the lower James River through the Elizabeth River. The Elizabeth River possesses four major branches of its own. The surface runoff from the adjacent watershed is the source of freshwater discharged to the Elizabeth River. According to the observations of Morse et al. (2011), the four major branches of the Elizabeth River (shown in Fig. 1(a)) are regarded as the source regions of the phytoplankton. We use the DS to represent the phytoplankton in order to study the transport of phytoplankton by the hydrodynamic field. The DS are simulated by passive tracers in a three-dimensional numerical model. It should be noted that the passive tracers cannot reproduce any biological processes of the reactive harmful algae blooms (HABs). The advantage of using tracers enables us to diagnose the physical processes that impact the transport of HABs. The spatial and temporal variations of the DS are examined under different hydrodynamic forcing condi-

tions. Our approach of using passive tracers can also be applied to other estuary and sub-estuary systems where water exchanges occur.

The paper is organized as follows. Section 2 describes the model and methods used in this study. In Section 3, model results are analyzed to present the distribution of DS under different forcing conditions. Section 4 discusses the correlation of external forcing field with the upriver transport of DS. Conclusions are presented in Section 5.

2 Numerical model and methods

2.1 Model description and configuration

A three-dimensional Hydrodynamic-Eutrophication Model (HEM-3D), developed by the Virginia Institute of Marine Science (Hamrick, 1992; Park et al., 1995), was used in this study. The model uses sigma vertical coordinates and curvilinear orthogonal horizontal coordinates. The vertical eddy viscosity/diffusivity coefficient was calculated by the Mellor and Yamada level 2.5 turbulence closure scheme (Mellor and Yamada, 1982; Galperin et al., 1988). This model had been used to reproduce the salinity, dissolved oxygen, and circulation successfully in the Chesapeake Bay (Hong and Shen, 2012, 2013) and the James River (Shen and Lin, 2006; Rice et al., 2012). Warner et al. (2005) indicated that the Mellor-Yamada closure scheme underestimates the vertical stratification in highly stratified systems. According to our previous model study, the HEM-3D model is reliable in modeling the stratification/destratification processes both in the Chesapeake Bay and the James River (Shen and Lin, 2006; Hong and Shen, 2012; Rice et al., 2012), suggesting that the Mellor-Yamada closure scheme is suitable for modeling the hydrodynamic process in the James River. To date, the HEM-3D has evolved over the past two decades to become one of the most used numerical models in estuaries (e.g., Hamrick and Wu, 1997; Park et al., 2005 ; Xia et al., 2007; Xu et al., 2008; Gong et al., 2009; Lee et al., 2011; Hong et al., 2016).

The model grid and computational domain is presented in Fig. 1(b). The model grids were designed to follow the main channel of the James River. The horizontal resolution of the model grids range from 30 to 900 m and the average resolution is about 200 m. A high resolution of grids was placed in the main channel of the James River and Elizabeth River to obtain the best representation of the topography in this area. The bathymetry of the James is based on the 90-m resolution of the NOAA coastal relief model. The Elizabeth River's is based on the 2002 survey provided by the Army Corps of Engineers. The model bathymetry is combined based on an historical survey. The James River bathymetry does not change much during the last 10 years based on current local surveys. There are 8 vertical sigma layers in the water column. Daily river discharges from three major rivers (marked in Fig. 1(b), river gauging stations maintained by the US Geological Survey) were included to provide the freshwater input into the James River. Only freshwater from local watersheds is discharged to the Elizabeth River as there is no large river in this sub-estuary area. Since major land use in Elizabeth River is urban, it is driven by precipitation and direct watershed runoff. The mean, minimum, and maximum river discharges to the headwaters of the James River are about 2.3×10^2, 0.1×10^2, and 32.8×10^2 m^3/s, respectively. The freshwater input to the Elizabeth River has the mean, minimum, and maximum values of 1.95×10^2, 0.03×10^2, and 37.6×10^2 m^3/s, respectively. Wind forcing data were obtained from the Norfolk Airport near Sewells Point (indicated by SP in Fig. 1(a)). The open boundary condition was obtained (in the format of one-way nesting) from a large domain model that simulated the real-time circulation in the entire Chesapeake Bay and validated by Hong and Shen (2012). The radiation open boundary condition is used for the DS so that the DS in the model domain can be freely transported out of the James River during ebb tide. For the inflow water, the DS concentration is set to zero since the inflow water is the bottom water of the Chesapeake Bay. Because the tracer was released inside the estuary, the DS concentration at the estuary mouth would vary depending on hydrodynamic conditions. In order to account for the DS re-entering the estuary during the flood tide, the model provided a linear interpolation of inflowing DS concentration based on the DS concentration at the end of the previous ebb tide and incoming DS concentration from the Chesapeake Bay (equal to zero in our case) for a specified time interval (about 1.2 hours based on the research of Shen and Haas (2004)). Model outputs are analyzed to investigate the transport processes between the James River and its sub-estuary, the Elizabeth River.

For the purpose of investigating the upriver transport in this estuary and sub-estuary system, passive tracers were continuously released from the four major branches of the Elizabeth River (marked in Fig. 1(a)) to represent the sources of the DS. The reason for designating these four major branches of the Elizabeth River as the source area of DS was based on the research of Morse et al. (2011), which concluded both from *in situ* observations and numerical study. By using passive tracers, we focused on exploring the physical effect on the transport of HABs. The effects of biological processes are not included. We aimed at quantitatively assessing the contribution of wind, river discharge, subtidal water level set-up/set-down at the entrance of the James River, and spring-neap tidal modulation on the transport of DS from the Elizabeth River to the upper James River. In order to obtain the best precondition for the realistic model simulation in year 2005, we use the forcing fields of 2004 and 2005 to run the

model continually for two years and only analyzed the second year (2005) for the DS transport.

2.2 Model calibration

The calibration of this James River model is presented in Fig. 2. The modeled salinity profiles were compared with observations obtained from the Chesapeake Bay Water Quality Monitoring Program. The typical runoff year 2005 was selected to present the results. There were 6 available stations covering both the main channel of the James River and the Elizabeth River (see Fig. 1(a) for the location of these stations). The vertical structures together with the seasonal variations that are shown in the measured salinity data were reproduced by the model simulation. Overall model simulated salinity structure was in good agreement with the observations. The tidal and subtidal water levels were compared at station Sewells Point (marked in Fig. 1 (a)) where the observations were available. Here the subtidal water level was calculated by removing the tidal signal from the raw data. Using a method of Wilmott (1981), we define Skill $= 1 - \sum (X_{\text{model}} - X_{\text{obs}})^2 / \sum \left(\left(X_{\text{model}} - \overline{X_{\text{obs}}} \right) + \left(X_{\text{obs}} - \overline{X_{\text{obs}}} \right) \right)^2$, where X is the variable being compared with a time mean $\overline{X}$. Perfect agreement between model results and observations will yield a skill value of one and complete disagreement yields a skill value of zero. The statistics of one year's water elevation comparison are shown in Table 1. The results indicated the model has good skill in simulating both the tidal and the subtidal elevations, and the better skill is obtained in the tidal simulation. As an example, water elevation comparisons during a randomly selected period are presented in Figs. 2(g) and 2(h). Model results matched the observations very well. These indicated that the model had robust response to external forcing and was reliable in simulating the hydrodynamic circulation in the James River.

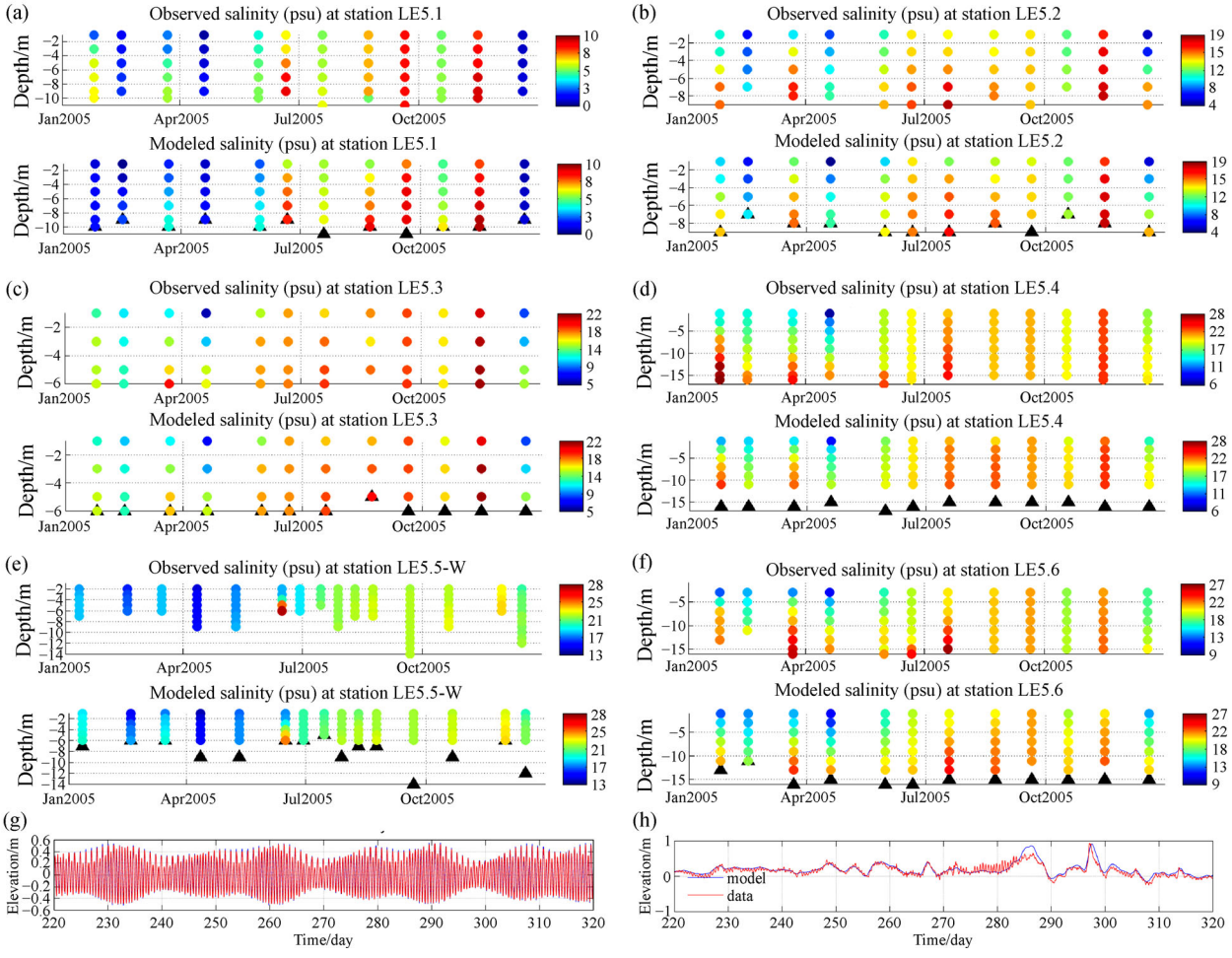

Fig. 2 (a–f) Model-data comparisons for the temporal variations of salinity profile at stations LE5.1, LE5.2, LE5.3, LE5.4, LE5.5-W, and LE5.6. The observations were obtained from the Chesapeake Bay Water Quality Monitoring Program; (g–h) comparisons of tidal and subtidal water elevation at Sewells Point station.

Table 1 Statistics of the model-data comparison in water level. RMS denotes root mean square

	Mean_obs	Std_obs	Mean_mod	Std_mod	RMS	Skill
Tidal	0.0002	0.2571	0.0002	0.2528	0.0512	0.9898
Subtidal	0.1243	0.1590	0.1851	0.1856	0.1397	0.8322

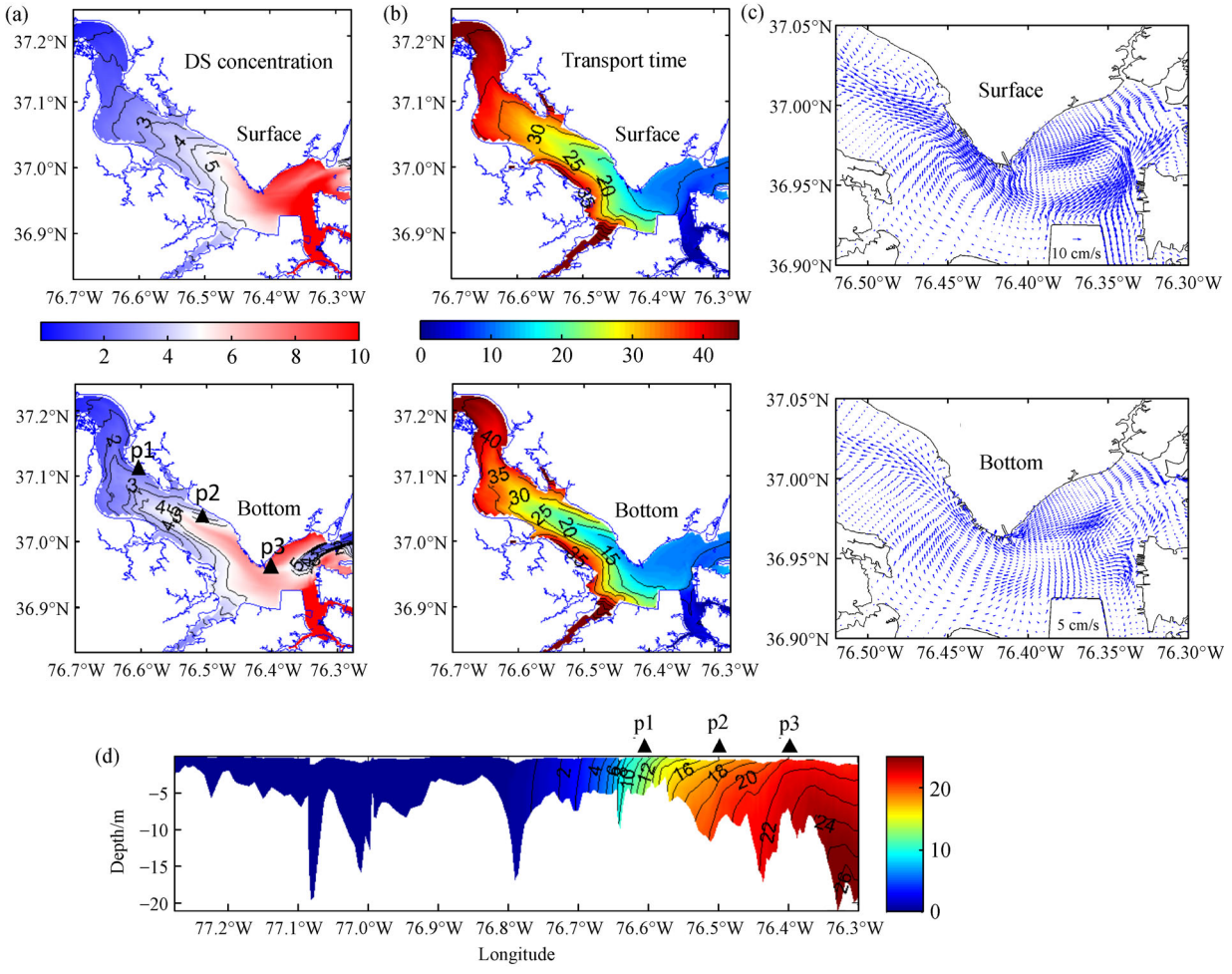

Fig. 3 Monthly mean results in August, 2005: (a) surface and bottom layer DS concentration (arbitrary unit); (b) surface and bottom layer DS transport time (day); (c) surface and bottom layer residual circulation; (d) salinity transect along the main channel of the James River. The location of the transect is marked in Fig. 1(b).

3 Results

3.1 Typical spatial feature of upriver transport

For the purpose of presenting the typical feature of DS upriver transport, the monthly mean DS concentration in August, 2005 is presented in Fig. 3(a). In the surface layer, the high DS concentration can be observed in the lower James River and along the coast of NNP. In the bottom layer, the DS can be transported further upstream. The high DS concentration appeared largely along the deep channel of the James River. The DS transport time is estimated by water age. Here the water age is defined to represent the average time that the water mass is being transported from the source area (four branches of the Elizabeth River) to the area of concern (Deleersnijder et al., 2001). The water age is governed by the following equations:

$$\frac{\partial C(t,x,y,z)}{\partial t} + \nabla\left(\vec{u}\,C(t,x,y,z) - K\nabla C(t,x,y,z)\right) = 0, \quad (1)$$

$$\frac{\partial \alpha(t,x,y,z)}{\partial t} + \nabla\left(\vec{u}\,\alpha(t,x,y,z) - K\nabla\alpha(t,x,y,z)\right) = C(t,x,y,z). \quad (2)$$

The mean water age can be calculated as follows:

$$a(t,x,y,z) = \frac{\alpha(t,x,y,z)}{C(t,x,y,z)}, \quad (3)$$

where $\nabla = \vec{i}\frac{\partial}{\partial x} + \vec{j}\frac{\partial}{\partial y} + \vec{k}\frac{\partial}{\partial k}$, $C(t,x,y,z)$ is the tracer concentration, $\alpha(t,x,y,z)$ is age concentration, $\vec{u}$ is the velocity field, and K is the diffusivity tensor. The boundary condition for the age tracer is same as those for the DS. The model was run for two years with real forcing to get the initial condition of the age tracer. Figure 3(b) shows the monthly mean water age in August. It indicates that it takes 15–20 days to transport DS from the Elizabeth River to the mesohaline portion of the James River. The transport time in the surface layer is about 3–5 days longer than that in the bottom layer, which means that estuarine circulation provides the major passage for transporting DS upstream near the bottom layer.

The monthly mean estuarine circulation in the lower James River is presented in Fig. (3). The typical 2-layer gravitational circulation (surface layer outflow and bottom layer inflow) appeared in both the Elizabeth River and the James River. The counterclockwise eddy in the lower James River can be clearly discerned in the surface layer (Fig. 3(c)). The size of the eddy is about 10 km, which is equivalent to the tidal exclusion in this area. The southern edge of the eddy is close to the Elizabeth River mouth, and the northern edge can reach Hampton Flats and flows towards NNP. The eddy connects the water from the Elizabeth River to the deep channel west of the James River mouth, where the DS can be transported to Hampton Flats by the eddy. The strength of the circulation varies during spring and neap tidal cycles. Both the period and intensity of the eddy increase during neap tide (Shen et al., 1999). Such residual eddies also exist in a tidal channel in Wassaw Sound, which are subject to bathymetry, coastlines, and advective nonlinearity (Li et al., 2006). A transect of monthly mean salinity along the James River main channel is presented in Fig. 3(d). The location of this transect is marked in Fig. 1(b). The Stations P1, P2, and P3 are used to mark the corresponding sites in Figs. 3(a), 3(b), and 3(d). Being a partially mixed estuary, the isohalines are nearly vertical in the area upstream from P1. The vertical salinity difference is about 1–3 psu in the mesohaline portion of the James River (from P1 to P3). Relatively strong stratification (the vertical salinity difference is about 5 psu) can be observed near the mouth of the James River where high salinity water intrudes into the estuary from the lower Chesapeake Bay. A weak front around P3 can be observed even from this monthly mean result.

3.2 Temporal variations of upriver transport

From the results shown in Fig. 3(a), the area in the mesohaline region of the James River can be selected to represent the intensity of the upriver transport. A domain marked in Fig. 1(b) is used for this purpose and named as domain M hereinafter. The volume mean DS concentration in the entire water column of domain M is calculated and shown in Fig. 4. The DS concentration shows obvious seasonal variation. High DS concentration appears in the summer, especially in August. Low DS concentration usually appears in spring and winter. Pulses of DS concentration increase/decrease can be observed year-round. The mean transport time of DS in the domain M is also calculated to estimate the average time needed for the DS being transported from the Elizabeth River to this area. The increase (decrease) of DS concentration is usually accompanied by the decrease (increase) of transport time. The correlation coefficient for these is –0.63 (at a 95% confidence level). It is worthwhile to assess the contribution of each forcing field that impacts the hydrodynamic conditions and thereby impacts the DS transport. It should be noted that linear correlation only account for 63% of variance. There are some parts of the DS variations are not

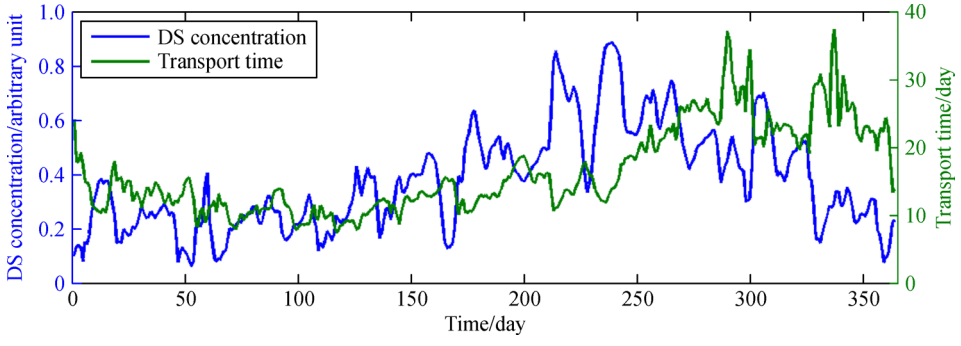

Fig. 4 Time series of volume mean DS concentration and transport time calculated in the entire water column of domain M. The location of domain M is marked in Fig. 1(b).

negatively correlated with the transport time, e.g., from Days 120 to 270, both the DS concentration and transport time show an increasing trend on a seasonal timescale. Such a trend could be caused by other factors. More research is needed to understand it.

3.3 Synoptic events analyses

3.3.1 Responses to the wind forcing

Wind forcing can strongly alter the estuarine circulation (e.g., Weisberg and Sturges, 1976; Wang and Elliot, 1978; Wong and Valle-Levinson, 2002; Narváez and Valle-Levinson, 2008). Figure 5(a) shows the wind vector observed at the Norfolk Airport close to Sewells Point in 2005. An abrupt change of wind direction can be observed around Day 281. Before Day 281, the southerly wind manifested for about 3–4 days and reached its maximum speed on Day 280. After Day 281, the northerly wind prevailed for approximately 10 days and reached its maximum speed around Day 287. The horizontal distributions of DS concentration during typically southerly (Day 280) and northerly (Day 287) winds are presented in Fig. 5(b). At Day 280, DS can be transported to the Hampton Flats area and upstream of the James River. At Day 287, the DS are confined near the mouth of the Elizabeth River. It clearly indicated that the southerly wind facilitated the DS transport from the Elizabeth River to the upper James River while the northerly wind acted to suppress such transport.

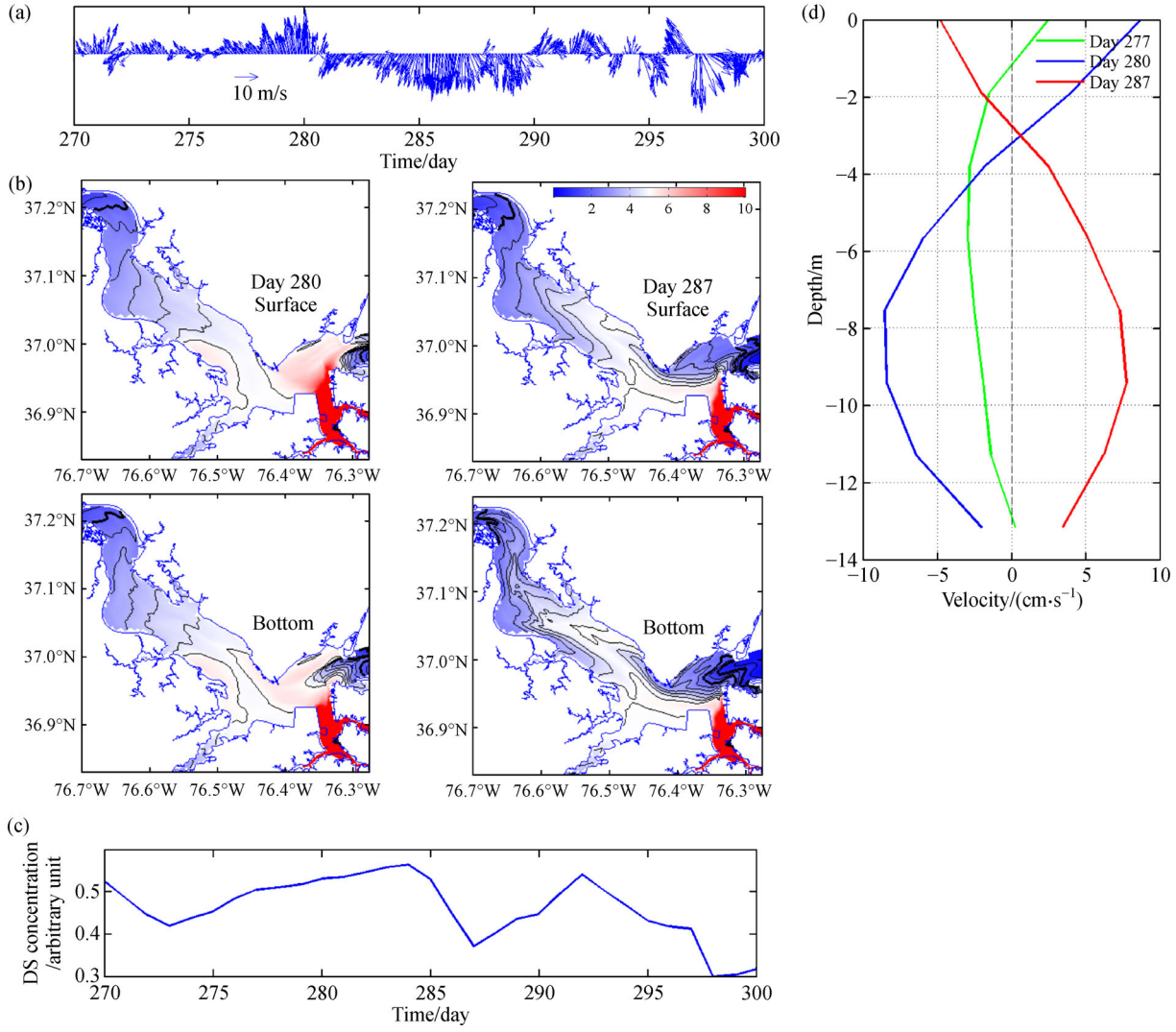

Fig. 5 (a) Wind vector from Day 270 to Day 300, 2005; (b) surface and bottom layer DS concentration (arbitrary unit) on Days 280 (southerly wind) and 287 (northerly wind); (c) time series of volume mean DS concentration in domain M; (d) exchange flow at the mouth of the Elizabeth River on Days 277, 280, and 287, respectively. The location of the exchange flow was marked in Fig. 1(a) by the green star at the Elizabeth River mouth. The positive (negative) direction indicates flow leaving (entering) Elizabeth River.

The time series of mean DS concentration in the domain M is plotted in Fig. 5(c). It indicates the DS concentration increases during the southerly wind condition. The DS concentration does not decrease immediately as the wind direction changes from southerly to northerly. It starts to decrease about 4 days later than the time of the northerly wind starts. Such a time lag may be due to the transport time needed for the DS being transported from the lower James to the mesohaline region. The residual velocity profiles at the Elizabeth River mouth are plotted in Fig. 5(d) to show the changes of exchange flow. The location of the exchange flow were marked in Fig. 1(a) by the green star at the Elizabeth River mouth. The positive (negative) direction means flow leaving (entering) the Elizabeth River. The exchange flow is greatly strengthened from Day 277 to Day 280. However, as shown on Day 287, the exchange flow can be totally reversed when the strong northerly wind prevails. The impact of wind will be discussed in detail in Section 4.

3.3.2 Responses to the pulse of water level

The remote effect of wind in the Chesapeake Bay can result in water level rise (set-up) or drop (set-down) at the entrance to the James (Shen and Gong, 2009). When water level set-up occurs, a unidirectional barotropic inflow is expected throughout the entrance of the estuary while a set-down can produce the opposite flow. We plotted the subtidal water level time series at the mouth of the James River in Fig. 6(a). Since this time series is the modeled result from a large domain model (Hong and Shen, 2012), we superimposed the observed subtidal water level that is only available from the Sewells Point Station (marked in Fig. 1(a)). The water level at the Sewells Point Station shows consistent variations with that at the James River mouth. The open boundary condition of the James River model was obtained (in the format of one-way nesting) from a large domain model that simulated the real-time circulation in the entire Chesapeake Bay. The water level pulse that appeared at the James River mouth is the remote wind forcing effect from the Bay. There is an abrupt subtidal water level pulse (with the amplitude around 0.8 m, see Fig. 6(a)) around Day 297 in 2005. The horizontal DS concentrations on Days 295, 298, and 301 are presented in Fig. 6(b) to show the effect of the water level pulse that occurred around Day 297. A remarkable change can be observed during and after the pulse. When the unidirectional barotropic inflow intrudes into the James River during the pulse, water from Chesapeake Bay occupied the large portion of the lower James River and the water in the Elizabeth River was confined in its local area. Right after the pulse, large amounts of DS are transported out of the Elizabeth River, while a portion entered the Chesapeake Bay. Most of the area of the lower James had high concentrations of DS. Another numerical experiment with local wind forcing turned off showed that the results were not too different from the results presented here. This indicated that the local wind effect was overwhelmed by the abrupt water level pulse at the James River mouth, which is consistent with the study of Shen and Gong (2009). Therefore, the relaxation of the water level pulse is the dominant factor that causes such a large domain upstream transport on Day 301. The pattern of DS distribution shown on Day 301 lasts for about a week and high DS concentrations expanded into a very large portion in the upper James River (as an example, see the result on Day 306, Fig. 6(b)), which suggests that remote wind forcing might be one of the important factors influencing the transport of phytoplankton from the Elizabeth River to the Upper James River and lower Chesapeake Bay.

The time series of mean DS concentration in the domain M (Fig. 6(c)) shows the DS reaches its minimum value around Day 298 and lasts about 2 days. It starts to increase from Day 300. In the domain M, the response of DS concentration to the water level pulse has a time lag of about 1 day, which is less than the time lag for the wind forcing effect. The residual velocity profiles at the mouth of the Elizabeth River are plotted (Fig. 6(d)). The exchange flow has a quick response to the sea level pulse. It is reversed at Day 297, the same day that the water level pulse occurs. The adjustment of the exchange flow is rapid. The recovered normal exchange flow is observed on Day 301 and strengthened on Day 308.

3.3.3 Response to the pulse of river discharge

The freshwater pulse often occurs in the estuary. A buoyancy change caused by an increase of freshwater discharge can alter the circulation, thus altering the transport of DS. Figure 7(a) presents the total river discharge from the head of the James River. As a typical subtropical river, the James River experiences its wet season in the spring and its dry season in the summer and autumn. There were four river discharge pulses in 2005. The pulse between Days 80 and 100 was selected to illustrate the response of DS transport. As seen in Fig. 7(b), the high flow around Day 94 can greatly suppress the upriver transport of DS and the DS can be transported into the Chesapeake Bay through the James River mouth. Day 258 was selected to show the DS distribution during the typical dry season. The water with high DS concentration can be transported to the upper James River and can occupy a very large area. With other factors such as the precondition of salinity inside the estuary and different forcing between these two days contributing, the results are not fully comparable between these two days. Nevertheless, the responses to the impact of typical high and low freshwater discharge are visible. In order to look into the

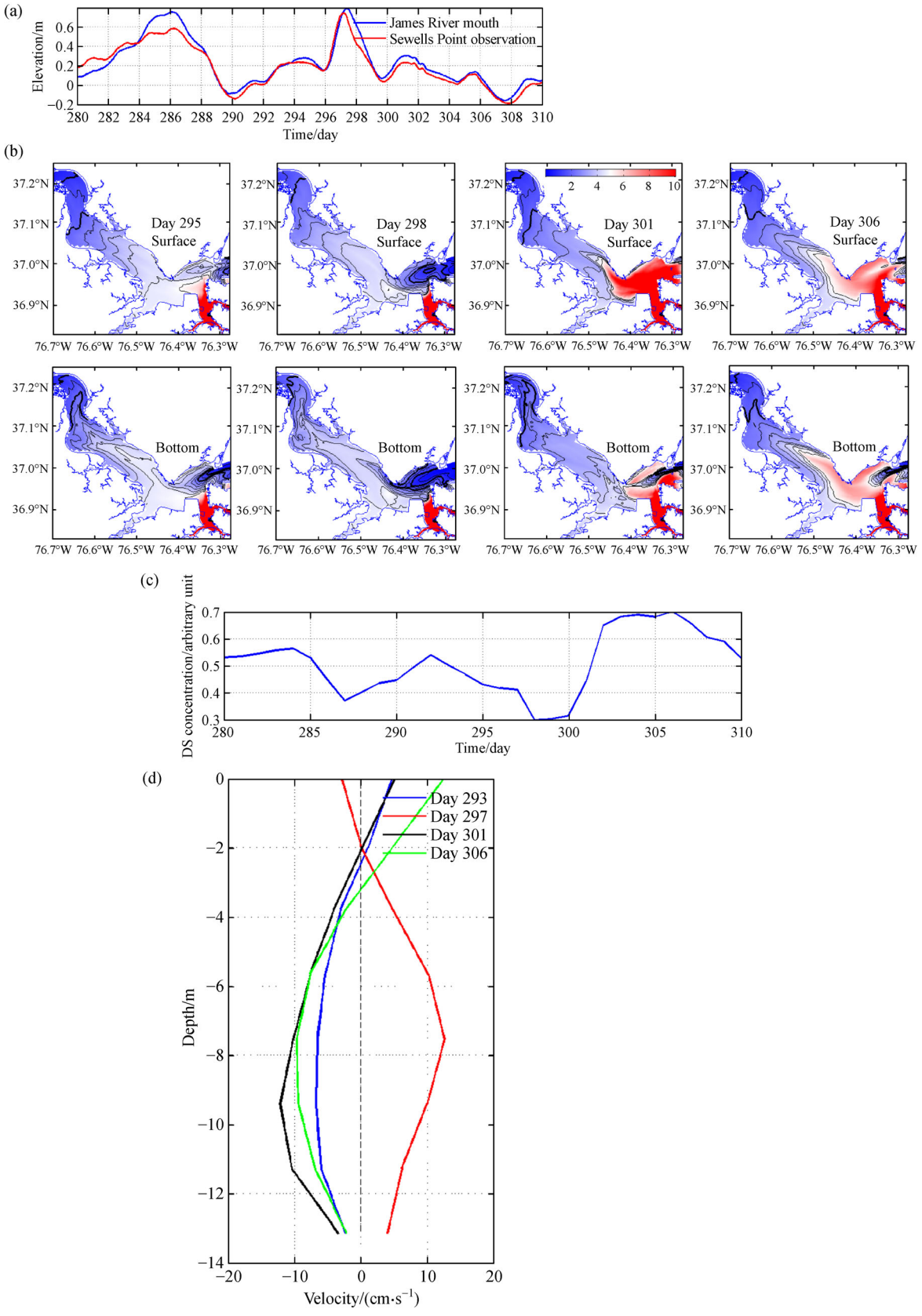

Fig. 6 (a) Subtidal water level at the mouth of the James River. The observed subtidal water level at Sewells Point station is also superimposed; (b) daily mean surface and bottom layer DS concentration (arbitrary units) on Days 295, 298, 301, and 306 in 2005, respectively; (c) time series of volume mean DS concentration in domain M; (d) exchange flow at the mouth of Elizabeth River on Days 293, 297, 301, and 306 in 2005, respectively.

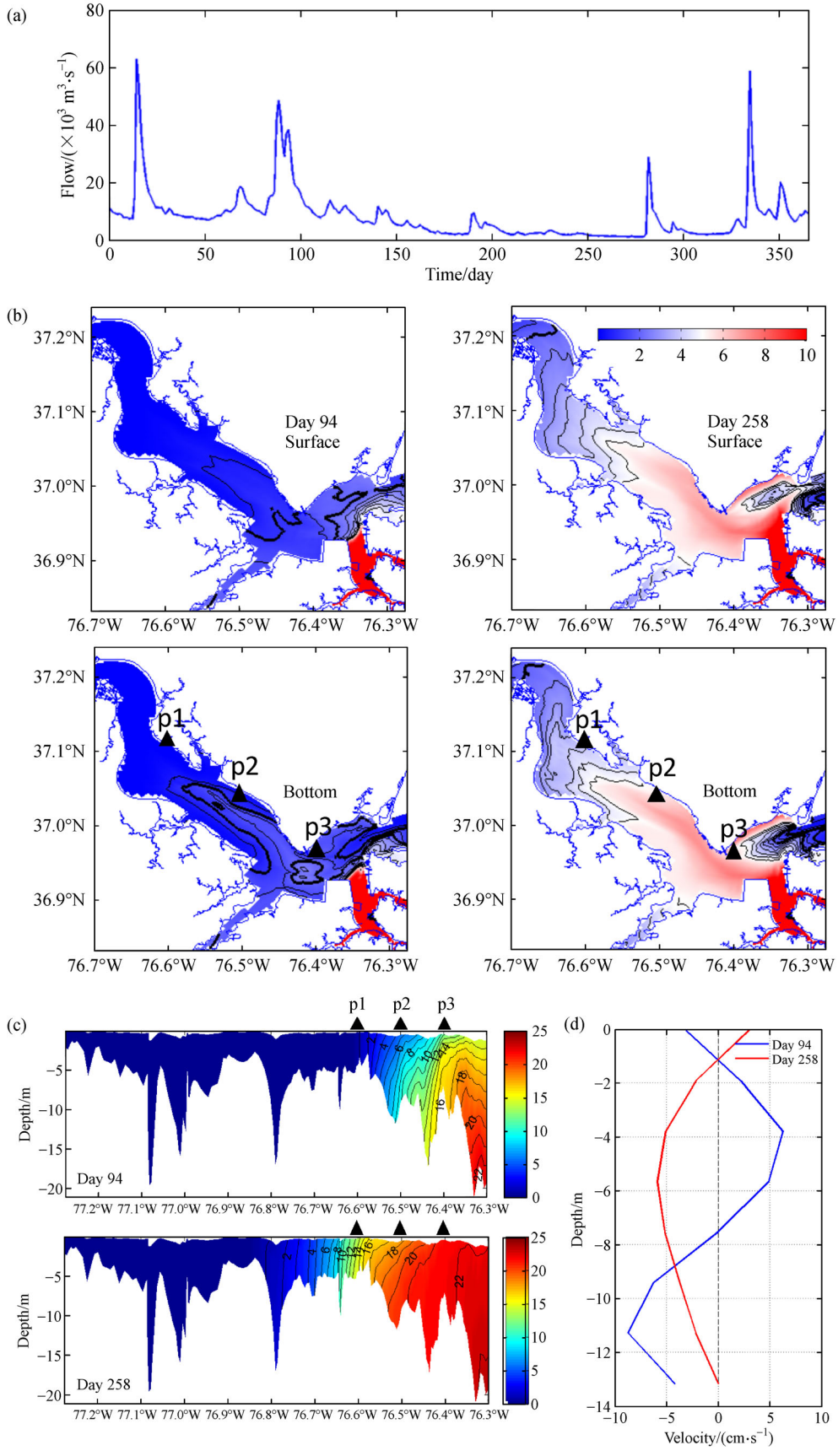

Fig. 7 (a) Total river discharge to the James River from its headwaters; (b) daily mean surface and bottom layer DS concentration (arbitrary unit) on Days 94 and 258 in 2005; (c) salinity transect on Days 94 and 258 along the main channel of the James River (see Fig. 1 (b) for the location of the transect. Here p1, p2, p3 represent the corresponding sites in (b) and (c)); (d) exchange flow at the mouth of Elizabeth River on Days 94 and 258, respectively.

vertical stratification, a salinity transect along the James River (location marked in Fig. 1(b)) was presented in Fig. 7 (c). The salt intrusion was pushed downstream by the river pulse around Day 94. The partially mixed condition at Day 258 resulted in the nearly identical DS distribution at the surface and bottom layers (Fig. 7(b)). The exchange flow profiles along the Elizabeth River mouth indicated that the 3-layered circulation appeared around Day 94 (Fig. 7(d)). During the river pulse period, there was flow into the Elizabeth River at both the surface and bottom layers. These inflows returned to the James River at mid-depth. The 3-layered circulation pattern was driven by the differences in the vertical salinity structure in the Elizabeth River and the adjacent James River. Such 3-layered circulation also appeared in the Baltimore Harbor, a sub-estuary in the upper Chesapeake Bay (Hong et al., 2010). It should be noted that this river pulse had two peaks and lasts for about two weeks. Such a strong and long-lasting river pulse is significant enough to deplete almost all of the DS in the mesohaline portion of the James River. Other weak and short-term river pulses might only weaken the upriver transport of DS slightly.

3.4 Characteristic responses of dissolved substances to the tidal effect

Tidal elevation shown in Fig. 8(a) has two spring-neap tidal periods from Day 208 to Day 240 in 2005. In the lower James River, the typical spring and neap tidal ranges are about 1 m and 0.6 m, respectively. In order to assess the tidal effect clearly, a numerical experiment with tidal forcing only was conducted. Wind forcing was excluded and constant annual mean river discharge was used. The model was run from Day 1 until Day 240. The fluxes of DS across the mouth of Elizabeth River were computed from the model outputs. The 25-hour average results shown in Fig. 8(b) indicate that the variations of the flux are driven by the spring-neap tidal variation. The flux was greatly decreased during the period from neap tide to spring tide and increased from spring tide to neap tide. The exchange flow along the mouth of the Elizabeth River is plotted in Fig. 8(c). We select Days 213 and 220, which represent the respective times when the minimum and maximum fluxes of DS across the Elizabeth River mouth occurred. The exchange flow on Day 220 is stronger than that on Day 213, as expected. A strong signal of spring-neap tidal modulation on the DS transport in this estuary and sub-estuary system is obvious. It should be noted that there are asymmetric variations of DS flux during the spring and neap tidal periods. Such asymmetry is due to the time lag that appeared in the variations of mass flux and the DS concentration field. The mass flux always reaches its maximum a few days before the maximum DS concentration appeared at the Elizabeth River mouth. The mean DS

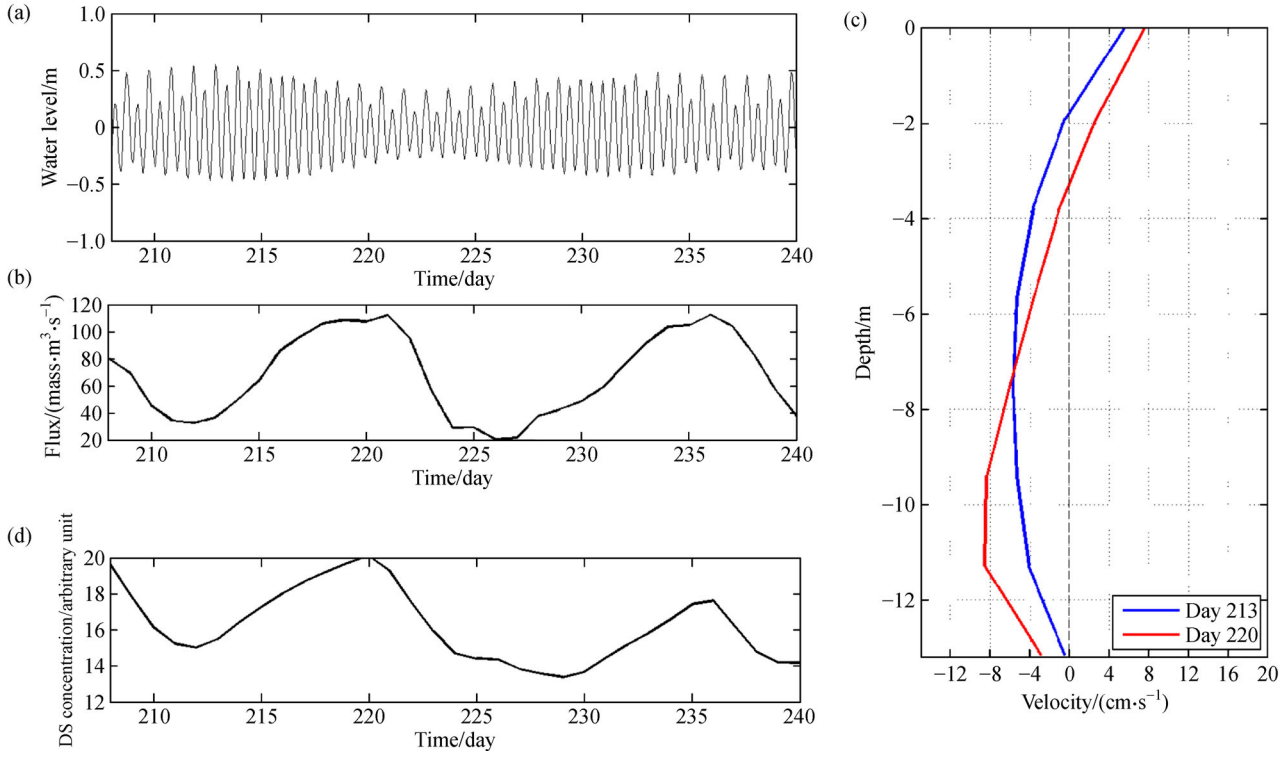

Fig. 8 (a) Time series of tidal elevation at Sewells Point Station in 2005; (b) low-pass filtered DS flux (mass×m^3/s, mass is in arbitrary units) across the mouth of Elizabeth River; (c) exchange flow at the mouth of Elizabeth River on Days 213 and 220, respectively; (d) volume mean DS concentration in the domain M.

concentration calculation in domain M is shown in Fig. 8 (d). The variation of mean DS concentration in domain M is nearly in the same phase as the DS flux across the Elizabeth River.

4 Analyses and discussion

4.1 Wind sensitivity

In order to assess the wind effect on the transport processes and isolate other forcing factors at the same time, idealized wind pulses from the north, west, south, and east were applied to the model. Wind and sea level fluctuations in coastal areas and estuaries are dominated by periods of ~2–7 days (Wong and Garvine, 1984). Statistically significant correlations among wind, sea level, and subtidal circulation have been found at those periods in the Chesapeake Bay region (Wong, 2002). The approximate summertime average wind speed over James River is roughly 5 m/s. The model was run for 230 days in total. The first 212 days were run without wind forcing. Then the wind pulse (5 m/s, from Days 213–215) from four different directions (north, west, south, and east) was added to the model for each run. Wind forcing was ramped up (down) for 10 hours at the beginning (end) of the pulse. The run without including the wind pulse is referred as the Base Run.

Flow across the Elizabeth River mouth is important in determining the DS flux across the mouth, which is helpful in evaluating the amount of DS that are injected into the James River. Figure 9(a) illustrates the residual velocity profiles across the mouth of the Elizabeth River. The positive (negative) value represents the water flowing out of (into) the Elizabeth River. All the results were sampled at Day 215. The two-layer circulation in the Elizabeth River was strengthened under the southerly and easterly winds forcing conditions. The southerly wind was in the downriver direction of the Elizabeth River. The study of Chen and Sanford (2009) indicated that the moderate down-estuary wind has a tendency toward increasing stratification by wind straining that dominates over direct wind mixing, which results in a strengthened two-layer exchange flow. The northerly and westerly winds act to weaken the exchange flow. The northerly wind reverses the surface flow, which results in the 3-layered circulation in the Elizabeth River (i.e., inflow in the surface and bottom layer, outflow in the mid-depth), which also appears in the case with the freshwater pulse. The resulting subtidal DS flux across the mouth of Elizabeth River is shown in Fig. 9(b). With the same wind speed, a different wind direction can cause remarkable change in the DS flux. The largest flux occurred during the southerly wind event and the flux was nearly tripled in comparison with the Base Run. The flux value under the southerly wind pulse is more

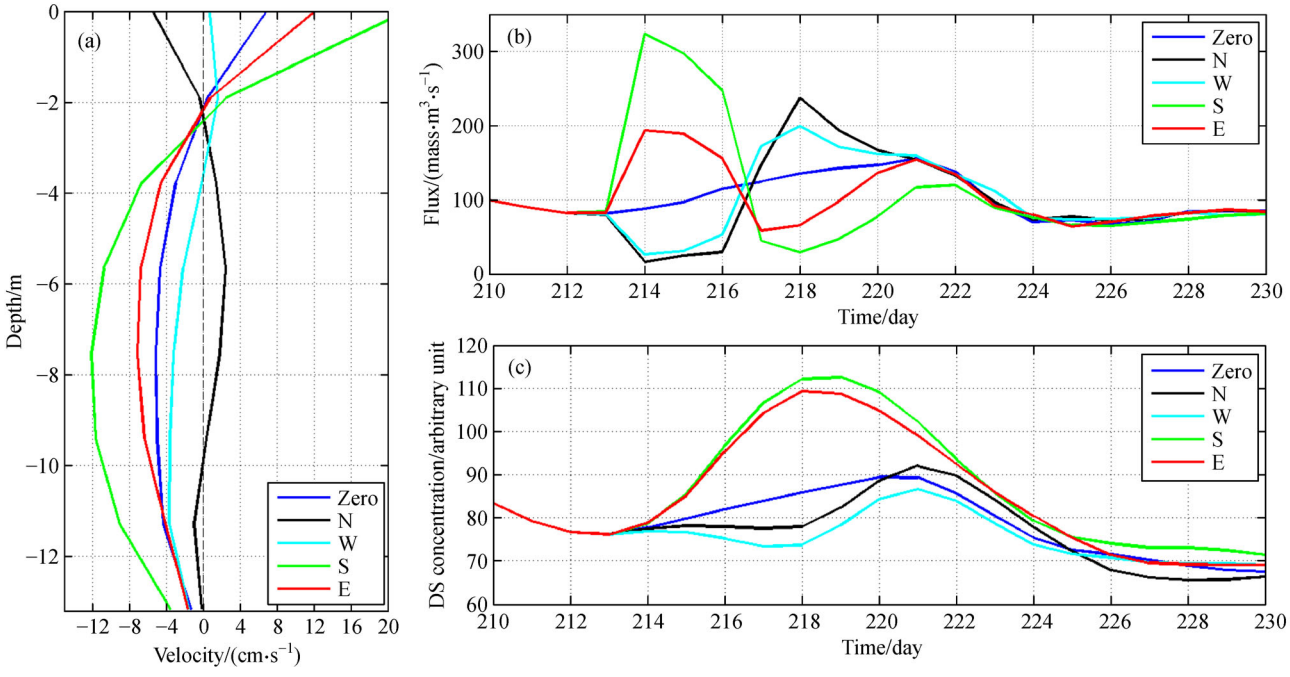

Fig. 9 Results from the sensitivity runs with wind turned off (Zero), northerly wind (N), westerly wind (W), southerly wind (S), and easterly wind (E), respectively: (a) exchange flow at the mouth of Elizabeth River; (b) flux of dissolved substances at the mouth of Elizabeth River, which were calculated from the transect across the mouth of Elizabeth River shown in Fig. 1(a); (c) volume mean DS concentration in the domain M.

than 6 times the value obtained under northerly and westerly winds. The system adjusted dynamically during and after the wind pulse. After the wind forcing disappeared, a flux rebound could be observed. Such rebound of flux is mainly caused by the adjustment of barotropic flow along the Elizabeth River, which results from the setup/setdown of the water level by wind pulse. The influence of wind lasted about 6–8 days. Under a real forcing condition, such a rebound cannot be discerned clearly, since the wind forcing varies continuously and will never really disappear.

Figure 9(c) shows the subtidal total DS concentration calculated over the water column in domain M. Remarkable increases of the DS concentration in the southerly and easterly wind forcing cases are observed, respectively. The increment is about one-third of the total DS concentration in the Base Run and the southerly wind can cause a higher increment than the easterly wind. The DS concentration decreases in the northerly and westerly wind but the decrement is relatively minor. The westerly wind can cause a higher decrement than the northerly wind. The maximum DS concentration increase/decrease occurs around Day 219, which is about 4 days later than the wind pulse event. The southerly and easterly winds facilitate the transport of DS to the Upper James River while the northerly and westerly wind act to suppress such transport.

4.2 Influences of dissolved substances releasing time

The results shown in Section 3.4 indicate that the spring and neap tidal modulation on the transport of DS is very prominent in the James River. If the DS entering the James River during a different tidal period (which signifies an instantaneous release of DS, unlike the continuous release simulated in the previous model runs), will they show a different spatial distribution pattern and a different transport time? In order to quantify the influence of releasing time, two experiments are conducted with passive tracers released from four branches of the Elizabeth River for 12 hours from 0:00 to 12:00, on Day 213 (spring tidal condition, Run Sp hereafter) and Day 220 (neap tidal condition, Run Ne hereafter), respectively. Only the manner of tracer release was changed. Other hydrodynamic settings of these two experiments are identical with those shown in Section 3.4.

Travel time corresponding to the depth-averaged peak concentration of DS is shown in Fig. 10. Here the travel time is defined as the first time when the local depth-averaged peak concentration appears after releasing. The times shown in Figs. 10(a) and 10(b) were relative to Days 213 and 220, respectively. If tracers were released during the spring tides (Fig. 10(a)), they were quickly transported to the lower James River and the area nearby the deep channel in the upper portion of the lower James River, usually within 10 days. But it took a much longer time for the DS to be transported to the area further up the James River. On the other hand, if tracers were released in the Elizabeth River during the neap tides (Fig. 10(b)), they took more time (at least 15 days) to be transported to the lower and upper portions of the James River. There were large areas in the James River that had travel time less than 20 days in Run Ne, which means the upriver transport can be extended to a larger domain within this timescale. However, it took more time for the DS to reach such a large

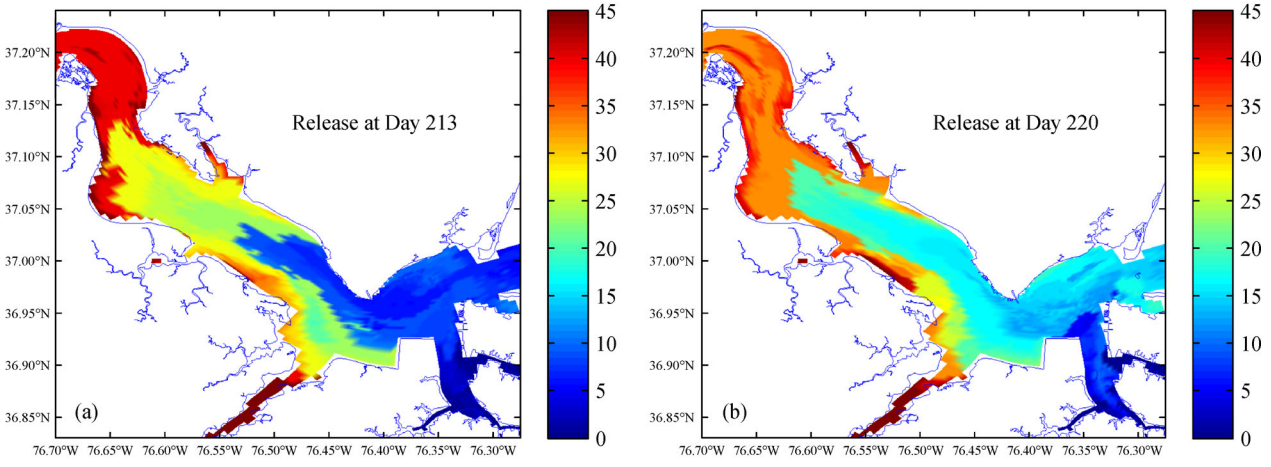

Fig. 10 Travel time (days) corresponding to the depth-averaged peak concentration of DS released from the four branches of the Elizabeth River on Day 213 (left) and Day 220 (right). The travel time is relative to the releasing day. Days 213 and 220 are selected to represent the typical spring and neap tidal condition, respectively.

spatial extent in Run Sp. The difference between Fig. 10(a) and Fig. 10(b) suggests that the dominant process of transporting DS maybe different in spring and neap tides. Since tidal flushing is stronger during the spring tide than during the neap tide, the tidal flushing may play an important role in transporting the DS during spring tide (Run Sp), which results in the shorter travel time in the lower part of the James River. The gravitational circulation is stronger as tidal amplitude decreases during the neap tide. The increase of bottom DS concentration along the deep channel during the neap tide can be discerned (figure not shown). As tidal flushing has a lesser contribution during neap tide than during spring tide, the travel time increases. The period and intensity of the counterclockwise eddy in the lower James River also increase during neap tide (Shen et al., 1999). The subduction along the frontal interface can transport more DS down to the bottom layer of the water column and may became a dominant process in transporting the DS to the upper James River during neap tide (Run Ne). Such a process is slower than tidal flushing, but can reach a larger area in the mesohaline region of the James River.

4.3 Relative importance of external forcing

Based on the results of this study, external forcing impacts the DS transport in different ways. It is necessary to assess the relative importance of the external forcing on modulating the upriver transport of DS. The time series of DS concentration averaged in domain M (as plotted in Fig. 4) is used to do the correlation analyses with external forcings. The corresponding correlation coefficients are listed in Table 2. The river discharge has the highest correlation coefficient (= – 0.71) in the yearly timescale. The correlation coefficients for the wind speed and subtidal water level at the entrance of the James River are –0.52 and 0.22, respectively. The relatively low correlation coefficients indicate that wind effect and subtidal water level can dominate the DS transport process in the synoptic timescale but have a less significant correlation in the yearly long timescale. The river discharge controls the seasonal variations of the DS upstream transport. Since the stratification is an important index to assess the estuary circulation and reflect the combined effect of external forcings, the stratification (calculated as the difference between bottom and surface salinity) at Station LE5.4 (a station near NNP) is selected to do the correlation with DS concentration averaged in the domain M. The correlation coefficient is –0.77, which is higher than the river discharge. A detide analysis was conducted for DS concentration, the average difference of DS concentration with and without tide is about 10%, suggesting that short-term tidal variation accounts for 10% of the variation.

The spectrum analyses of each variable listed in Table 2 were conducted using their daily means. The results are presented in Fig. 11. From the spectrum analyses, we find the dominant frequencies of each variable and the same significant frequency between DS concentration and other forcing variables, which identify the consistent response of DS transport to the variations of external forcing. Figure 11(a) shows the DS concentration has significant frequencies of 22.75, 28, and 14.56 days (in the sequence of significance). Comparing with the results of other variables, it can be seen that the consistent significant frequencies can be found. For example, the stratification has significant frequencies of 28, 14.56, and 22.75 days. The variations of DS transport show good response to the perturbations of stratification. This is consistent with the result in Table 2 that DS concentration and stratification has a high correlation. The significant frequencies for the subtidal water level are 23, 13, and 9 days. The significant frequencies for the river discharge are 24, 36, and 15 days. The significant frequencies for wind speed are 3, 6, and 10 days. The results indicate that variation of DS responses to the external forcings occur. Because each forcing has different timescale, a weak linear correlation can be expected for individual forcing due to the nonlinear effect.

The time series of the variables shown in Table 2 are used to do the multi-variable regression for the DS concentration and are compared with the model calculated results in Fig. 12. The variable matrix includes wind components, stratification, subtidal water level, and river discharge. A 15-day moving average was applied to all the data to remove the spring-neap tidal effect. The statistical significant correlation was obtained ($r = 0.858$, $p = 0.00001$). The regression result can account for 74% of the variance of the model result. Because the estuary responds to different forcing with different response times, sometimes a shift of peak concentration between regression results and model results can be observed. From these results, we can largely predict the subtidal variations of DS upstream transport based on the observations of the external forcing. When the condition is favorable for the upstream transport, HABs in the mesohaline region following the bloom in the Elizabeth River can be expected.

Table 2 Correlation coefficient (at 95% confidence level) of the mean DS concentration in domain M with each physical forcing component. The dominant tides in James River is M2 and S2. The 15-day running average is applied in order to remove the tidal effect from the one-year results

	River discharge	Wind speed	Subtidal water Level (Remote wind effect)	Stratification
Correlation coefficient	–0.71	–0.52	0.22	–0.77

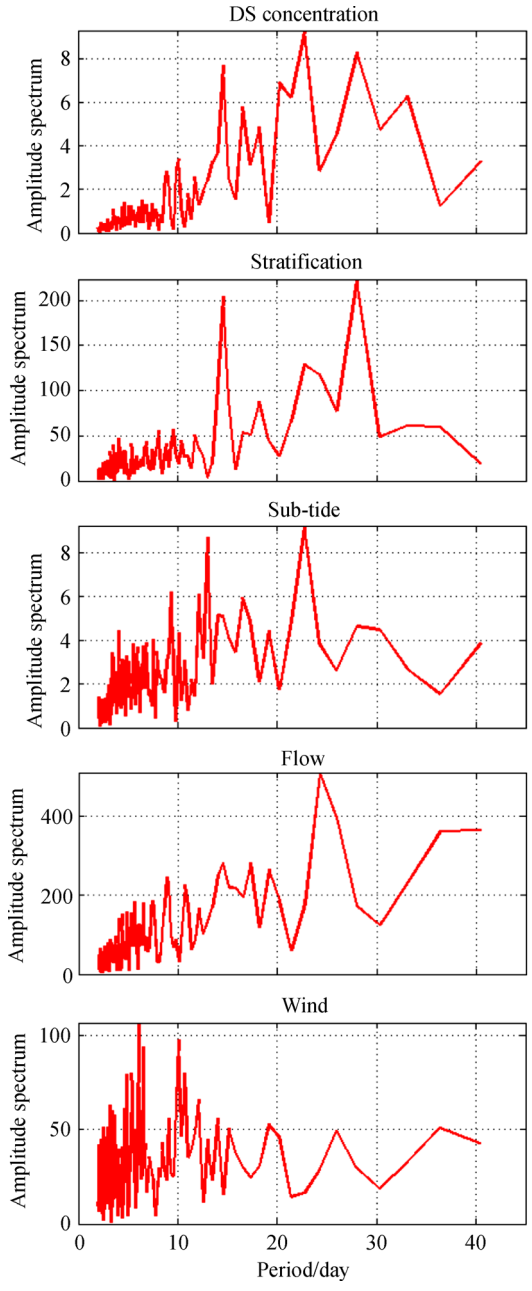

Fig. 11 Results of spectrum analysis for daily mean DS concentration and forcing variables. The first three significant frequencies for DS concentration are 22.75, 28, and 14.56 days.

5 Conclusions

Transport of water and waterborne materials are closely related to the physical processes that control the temporal-spatial variations of the concentration and the extent of upriver transport of DS. In this study, the four branches of the Elizabeth River are regarded as the source ground of phytoplankton initiation in the James River. Passive tracers are used to simulate the transport of phytoplankton by hydrodynamic circulation. The biochemical processes of phytoplankton are not included in the model in order to diagnose the impact of physical processes on the transport.

The hydrodynamic circulation in 2005 was reproduced by the HEM-3D. Together with several process-oriented numerical experiments, we found that the upriver transport of DS in this estuary and sub-estuary system is sensitive to external forcings and responds in different ways. The DS transport has a strong seasonal variation. More DS will be transported to the mesohaline region of the James River during the dry season, especially in August, than during the wet season. The transport time ranges from 15–30 days for the DS being transported from the Elizabeth River branches to the mesohaline portion of the James River. A large transport time occurs from September to December.

The exchange between the Elizabeth River and the James River is very sensitive to the synoptic events. The southerly/easterly wind, low river discharge, and neap tidal conditions all act to strengthen the exchange flow between the James and Elizabeth Rivers. On the other hand, the northerly/westerly wind, large river pulse, water level pulse, and spring tidal conditions act to reduce the exchange flow. The exchange flow can even be reversed under the northerly wind, high river pulse, and water level pulse conditions. When the exchange flow is strengthened, the upstream transport of DS increases and vice versa. The increased barotropic inflow caused by the water level pulse confined the exchange between the Elizabeth River and the James River. Right after the pulse, large amounts of DS were transported to the James River and lower Chesapeake Bay. The transport of DS to the upper James River can be greatly enhanced after the retreat of the water level pulse. The effect of the water level pulse can overwhelm the local wind forcing on controlling the exchange between the Elizabeth River and the James River. The strong and long-lasting river pulse can totally clean the DS in the upper portion of the lower James River. The weak and short-term river pulse has a minor effect on the upriver transport of DS in the lower James River. Owing to the needed transport time for the upstream transport, a 4-day time lag in response to the change of forcing is observed under the synoptic wind forcing event. For the water level pulse event, such a time lag is about 1 day.

The flux of DS across the Elizabeth River mouth was greatly decreased (increased) during the spring (neap) tidal period. The upriver transport of DS was much stronger during neap tide. However, tidal flushing plays an important role in transporting the DS during spring tide, which results in the shorter travel time in the lower part of the James River. The correlation analyses indicate that the river discharge is the dominant forcing for the long-term variation on the DS upstream transport. The wind forcing impacts the DS transport in synoptic timescales. The stratification in the lower James River is found to have a good correlation with the DS concentration in the domain M. By using these physical forcing fields, the physical forcing field can be used to largely predict the DS

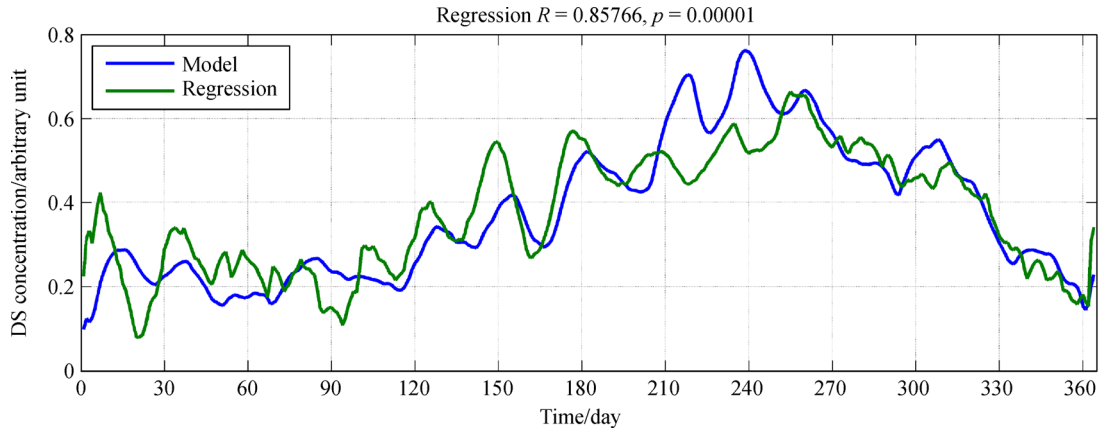

Fig. 12 (a) Multi-variable regression of DS concentration in the domain M with the forcing field, which include wind, water level, river discharge, and stratification at Station LE5.4 (near NNP and is maintained by the Chesapeake Bay Water Quality Monitoring Program). The correlation coefficient is 0.856 (p = 0.00001).

concentration variation in the mesohaline region of the James River (r = 0.858, p = 0.00001).

Acknowledgements This research was funded by the National Natural Science Foundation of China (Grant Nos. 41406005 and 41666001), Key Research Program of Frontier Sciences, CAS (No. QYZDJ-SSW-DQC022), and the Fundamental Research Funds for the Central Universities of SCUT under Grant No. 2017ZD101. Parts of this study were supported by the Virginia Department of Environmental Quality (contracts # 15050 and 14835). The development of the model was supported by USGS Project of Model Study of Change in Salinity under Different Sea-level Rise Scenarios in the York River and James River. We appreciate two anonymous reviewers' comments and constructive suggestions, which improve the manuscript. We thank Mac Sisson for his comments on the early version and help on editing the manuscript. This is the contribution number #3704 of Virginia Institute of Marine Science, College of William and Mary.

References

Basdurak N B, Valle-Levinson A (2013). Tidal variability of lateral advection in a coastalplain estuary. Cont Shelf Res, 61–62: 85–97

Brubaker J M, Simpson J H (1999). Flow convergence and stability at a tidal estuarinefront: acoustic Doppler current observations. J Geophys Res, 104(C8): 18257–18268

Chen S N, Sanford L P (2009). Axial wind effects on stratification and longitudinalsalt transport in an idealized partially mixed estuary. J Phys Oceanogr, 39(8): 1905–1920

Deleersnijder E, Campin J M, Delhez E J M (2001). The concept of age in marine modeling. I. Theory and preliminary model results. J Mar Syst, 28: 229–267

Galperin B, Kantha L H, Hassid S, Rosati A (1988). A quasi-equilibrium turbulent energy model for geophysicalflows. J Atmos Sci, 45(1): 55–62

Gong W P, Shen J, Hong B (2009). The influence of wind on the water age in the tidal Rappahannock River. Mar Environ Res, 68(4): 203–216

Hamrick J M (1992). A Three-Dimensional Environmental Fluid Dynamics Computer Code: Theoretical and Computational Aspects. Special Report in Applied Marine Science and Ocean Engineering. No. 317. Virginia Institute of Marine Science, College of William and Mary, Gloucester Point, Virginia

Hamrick J M, Wu T S (1997). Computational design and optimization of the EFDC/HEM3D surface waterhydrodynamic and eutrophication models. In: Delich G, Wheeler M F, eds. Next Generation Environmental Modelsand Computational Methods. Society for Industrial and Applied Mathematics, Pennsylvania,143–161

Hong B, Gong W, Peng S, Xie Q, Wang D, Li H, Xu H (2016). Characteristics of vertical exchange process in the Pearl River Estuary (PRE). Aquat Ecosyst Health Manage, 19(3): 286–295

Hong B, Panday N, Shen J, Wang H V, Gong W, Soehl A (2010). Modeling water exchange between Baltimore Harbor and Chesapeake Bay using artificial tracers: seasonal variations. Mar Environ Res, 70(1): 102–119

Hong B, Shen J (2012). Responses of estuarine salinity and transport processes to potential future sea-level rise in the Chesapeake Bay. Estuar Coast Shelf Sci, 104–105: 33–45

Hong B, Shen J (2013). Linking dynamics of transport timescale and variations of hypoxia in the Chesapeake Bay. J Geophys Res, 118: 1–13

Kuo A Y, Byrne R J, Brubaker J M, Posenau J H (1988). Vertical transport across an estuary front. In: Dronkers J, van Leussen W, eds. Physical Processes in Estuaries. New York: Springer-Verlag Berlin Heidelberg, 93–109

Kuo A Y, Byrne R J, Hyer P V, Ruzecki E P, Brubaker J M (1990). Practicalapplication of theory for tidal-intrusion fronts. J Waterw Port Coast Ocean Eng, 116(3): 341–361

Lee S B, Birch G, Lemckert C J (2011). Fieldand modeling investigations of fresh-water plume behavior in response to infrequent high-precipitation events, Sydney Estuary, Australia. Estuar Coast Shelf Sci, 92(3): 389–402

Li C, Armstrong S, Williams D (2006). Residual eddies in a tidal channel. Estuaries Coasts, 29(1): 147–158

Mellor G L, Yamada T (1982). Development of a turbulence closure model for geophysical fluid problems. Rev Geophys Space Phys, 20 (4): 851–875

Morse R E, Shen J, Blanco-Garcia J L, Hunley W S, Fentress S, Wiggins M, Mulholland M R (2011). Environmental and physical controlson the formation and transport of blooms of the dinoflagellate cochlodinium polykrikoides margalef in lower Chesapeake Bay and its tributaries. Estuaries Coasts, 34(5): 1006–1025

Narváez D A, Valle-Levinson A (2008). Transverse structure of wind-driven flow at the entranceto an estuary: Nansemond River. J GeophysRes, 113(C9): C09004

Park K, Jung H S, Kim H S, Ahn S (2005). Three-dimensional hydrodynamic and eutrophication model (HEM-3D): application to Kwang-Yang Bay, Korea. Mar Environ Res, 60(2): 171–193

Park K, Kuo A Y, Shen J, Hamrick J M (1995). A three-dimensional hydrodynamic eutrophication model (HEM-3D): description of water quality and sediment process submodels. Special Report in Applied Marine Science and Ocean Engineering. No. 327. Virginia Institute of Marine Science, Gloucester Point, VA 23062

Rice K C, Hong B, Shen J (2012). Assessment of salinityintrusion in the James and Chickahominy Rivers as a result of simulated sea-level rise in Chesapeake Bay, East Coast, USA. J Environ Manage, 111: 61–69

Shen J, Boon J D, Kuo A Y (1999). A modeling study of a tidal intrusion front and its impact on larval dispersion in the James River estuary, Virginia. Estuaries Coasts, 22(3): 681–692

Shen J, Gong W (2009). Influence of model domain size, wind directions and Ekman transporton storm surge development inside the Chesapeake Bay: a case study of extra-tropical cyclone Ernesto, 2006. J Mar Syst, 75(1–2): 198–215

Shen J, Haas L (2004). Calculating age and residence time in the tidal York River using three-dimensional model experiments. Estuar Coast Shelf Sci, 61(3): 449–461

Shen J, Lin J (2006). Modeling study of the influences of tide and stratification on age of water in the tidal James River. Estuar Coast Shelf Sci, 68(1–2): 101–112

Valle-Levinson A, Wong K C, Lwiza K M (2000). Fortnightly variability in the transverse dynamics of a coastal plain estuary. J Geophys Res, 105(C2): 3413–3424

Wang D P, Elliott A J (1978). Nontidal variability in the Chesapeake Bay and the Potomac River, evidence for nonlocal forcing. J Phys Oceanogr, 8(2): 225–232

Warner J C, Geyer W R, Lerczak J A (2005). Numerical modeling of an estuary: a comprehensive skill assessment. J Geophys Res, 110(C5): C05001

Weisberg R H, Sturges W (1976). Velocity observations in the west passage of Narragansett Bay: a partially mixed estuary. J Phys Oceanogr, 6(3): 345–354

Wong K C (2002). On the wind-induced exchange between Indian River Bay, Delaware and the adjacent continental shelf. Cont Shelf Res, 22 (11–13): 1651–1668

Wong K C, Garvine R W (1984). Observations of wind-induced subtidal variability inthe Delaware estuary. J Geophys Res, 89(C6): 10589–10597

Wong K C, Valle-Levinson A (2002). On the relative importance of the remote and local wind effects on the subtidal exchange at the entrance to the Chesapeake Bay. J Mar Res, 60(3): 477–498

Wilmott C J (1981). On the validation of models. Physical Geography, 2: 184–194

Xia M, Xie L, Pietrafesa L J (2007). Modeling of the Cape Fear River estuary plume. Estuariesand Coasts, 30(4): 698–709

Xu H, Lin J, Wang D (2008). Numerical study onsalinity stratification in the Pamlico River Estuary. Estuar Coast Shelf Sci, 80(1): 74–84